Application of a Gaussian Distribution Function To Describe Molecular UV−Visible Absorption Continua. 2. The UV Spectra of $RO_2^•$ Radicals

D. Marić*

Institut für Sicherheitstechnologie, P.O. Box 101564, D-50455 Köln, Germany

J. N. Crowley

Division of Atmospheric Chemistry, Max-Planck-Institut für Chemie, P.O. Box 3060, D-55020 Mainz, Germany

J. P. Burrows

Institut für Umweltphysik der Universität Bremen, P.O. Box 330440, D-28334 Bremen, Germany

Received: June 12, 1996; In Final Form: January 31, 1997[⊗]

The suitability of Gaussian distribution functions to describe the shape and temperature dependence of the UV absorption continua of peroxy radicals has been investigated. The ethylperoxy radical was used as a test case. Its 298 K absorption continuum was found to be best described by a semilogarithmic Gaussian distribution function. A linear Gaussian distribution function performed less well but still adequately described the continuous absorption. The temperature dependence of the ethylperoxy radical UV absorption continuum was also well predicted. Analogous results obtained for the methylperoxy radical support these conclusions. A theoretical comparison of the semilogarithmic and linear Gaussian distribution functions is given and a potential energy diagram of the ethylperoxy radical derived. The experimentally determined absorption cross sections of $HO_2^•$ have been reanalyzed. It is shown that either the measurements at short wavelengths are in error or an unidentified electronic transition of $HO_2^•$ exists.

1. Introduction

The hydroperoxy radical, $HO_2^•$, and organic peroxy radicals, $RO_2^•$, are important intermediates in both combustion processes and atmospheric chemistry. Recent reviews[1,2] have summarized the available kinetic and spectroscopic data for peroxy radicals and highlighted their importance as atmospheric trace species. Organic peroxy radicals are formed in the atmosphere predominantly by abstraction of hydrogen atoms from naturally occurring and anthropogenic hydrocarbons such as CH_4. Peroxy radicals are sufficiently reactive to undergo a large number of reactions with trace gases such as NO_x and ClO_x and with other $RO_2^•$. They play a key role in catalytic cycles that destroy O_3 in the stratosphere and generate or destroy O_3 in the troposphere depending on the NO_x concentration. Finally, they assist transport of NO_x to remote areas and play a vital role in photochemical smog formation.[3−5]

The role of peroxy radicals in the chemistry of the atmosphere can only be assessed provided that their reactions with other trace gases have been characterized by laboratory kinetic investigations. UV absorption spectroscopy has been found to be widely applicable as a detection method for both organic peroxy radicals and $HO_2^•$, and the vast majority of kinetic data have been gathered using this detection technique.

Although all peroxy radicals display in the wavelength region between 200 and 300 nm relatively intense, broad, featureless UV absorption continua assigned to a $(2)^2A'' \leftarrow (1)^2A''$ transition, the measurement of absolute cross sections has proved difficult even at room temperature.[1] Such difficulties are associated with the quantitative, *in situ* generation of pure samples of $RO_2^•$, which may be contaminated with strongly absorbing products of the $RO_2^•$ self-reaction (including $HO_2^•$) or other impurities introduced by the photolytic initiation of the chemistry. Some means to predict the shapes and temperature dependencies of the $HO_2^•$ and $RO_2^•$ absorption continua is therefore required to complement these experimental investigations and provide an additional approach for the analysis of spectra.

LeRoy *et al.*[6] described in detail the inversion of experimentally determined absorption continua of diatomic molecules to radial potentials and *vice versa* at any desired temperature. Nowadays such inversions are readily feasible as a consequence of the recent availability of fast personal computers. For some polyatomic molecules, including, for example, the peroxy radicals, the inversion can be performed assuming that the essential features of the molecule can be treated in terms of quasi-diatomic potentials, thus effectively avoiding complications arising from additional degrees of freedom.[7] However, in the case of peroxy radicals a computationally simpler method of spectral analysis is desirable and justified.

In the following we discuss Gaussian distribution functions, which in combination with the method of spectral moments and the reflection method provide a simple means for the analysis of peroxy radical spectra. The suitability of the method is tested by comparing and contrasting predictions with experimentally derived spectra. The ethylperoxy radical, $CH_3CH_2O_2^•$, has been selected for test purposes.[8,9] This choice was governed by a recent measurement of the UV absorption continuum of $CH_3CH_2O_2^•$ that has been obtained using diode-array absorption spectroscopy[8] and which arguably represents the most accurately measured $RO_2^•$ gas-phase spectrum to date (*cf.* ref 1 for details). The results thus obtained are compared with those for the methylperoxy radical, $CH_3O_2^•$.[1,2,10] The usefulness of Gaussian distribution functions for detecting unexpected features in the shapes of experimentally determined absorption continua will be addressed.

2. Assessment of Previous Investigations

Hitherto the shape and the temperature dependence of the absorption continua of peroxy radicals have been computed via

[⊗] Abstract published in *Advance ACS Abstracts,* March 15, 1997.

S1089-5639(96)01715-X CCC: $14.00

an *ab initio* method only for $HO_2^{\bullet}$.[7] In contrast, Lightfoot *et al.*[1] adopted a semiempirical method advocated by Marić *et al.*,[11] which describes the shapes of UV absorption continua via semilogarithmic Gaussian distribution functions and predicts their temperature dependencies in a manner originally described by Sulzer and Wieland:[12]

$$\sigma(T) = \sigma_{max}(T) \exp\{-a(T)[\ln(\tilde{\nu}/\tilde{\nu}_{max})]^2\} \qquad (1)$$

where $\sigma_{max}(T) = \sigma_{max}(0)\sqrt{\tanh}$; $a(T) = a(0)$ tanh; and tanh = $\tanh[hc_0\omega_e''/(2kT)]$.

In eq 1 the cross section and the wavenumber at the absorption maximum, $\sigma_{max}(T)$ and $\tilde{\nu}_{max}$, and the breadth parameter $a(T)$ are determined by fitting and, where more than one reaction component absorbs, deconvolution in an appropriate number of individual bands. Provided that the harmonic vibrational wavenumber ω_e'' is known, $\sigma_{max}(0)$ and $a(0)$, which are the values of the corresponding parameters at 0 K, can be computed, whereas $\tilde{\nu}_{max}$ does not depend on temperature in this model. Consequently, the shape of an UV absorption continuum can be predicted via eq 1 for any arbitrary temperature for which the underlying assumptions are reasonably valid. The theoretical justification of eq 1 was given by Marić and Burrows.[13] Finally, note that in eq 1 the maximum and median absorption coincide (*i.e.* $\sigma_{max}(T) = \sigma_{med}(T)$ and $\tilde{\nu}_{max} = \tilde{\nu}_{med}$), the latter being defined via $\int_0^{\tilde{\nu}_{med}} \sigma(T)\, d\ln(\tilde{\nu}) = \int_{\tilde{\nu}_{med}}^{\infty} \sigma(T)\, d\ln(\tilde{\nu}) = hB/2$, where B is the Einstein absorption coefficient.[14,15]

Lightfoot *et al.*[1] showed that eq 1 adequately describes the shapes of the absorption continua of at least 15 $RO_2^{\bullet}$ radicals at room temperature, the only exceptions being $HO_2^{\bullet}$ and $CH_3O_2^{\bullet}$. The shape of the absorption continuum of $HO_2^{\bullet}$ reported by Crowley *et al.*[16] could not be described via eq 1 in terms of a single band, whereas for $CH_3O_2^{\bullet}$ the shape of each reviewed absorption continuum was found to be accurately described via eq 1, but the combined data scattered in such a manner that they could not be fitted.[1] Subsequently, Crowley and Moortgat[17] used eq 1 to deconvolute the absorption continua of $BrCH_2CH_2O_2^{\bullet}$ and $BrCH(CH_3)CH(CH_3)O_2^{\bullet}$ from that of $HO_2^{\bullet}$ at 298 K. Fenter *et al.*[9] observed that eq 1 correctly describes the shapes of the absorption continua of $CH_3O_2^{\bullet}$ at 298 and 662 K and $CH_3CH_2O_2^{\bullet}$ at 298 and 600 K. The predicted temperature dependence of $a(T)$ agreed with that determined experimentally, whereas for $\sigma_{max}(T)$ the comparison was inconclusive because of experimental difficulties.[9] Catorie *et al.*[18] used eq 1 to describe the shape of the absorption continuum of $ClCH_2O_2^{\bullet}$ at 298, 464, and 588 K, but they did not compare the predicted temperature dependence. More recently, Catoire *et al.*[19] described via eq 1 the shapes of the absorption continua of $Cl_2CHO_2^{\bullet}$ and $Cl_3CO_2^{\bullet}$ at 298 K. In addition, Huie and Clifton[20] found that eq 1 adequately describes the shape of the absorption continuum of $HOCH_2O_2^{\bullet}$ in the aqueous phase at room temperature. Equation 1 was successfully used to describe the shapes and predict the temperature dependencies of the absorption continua of Cl_2,[11,13,21] Br_2,[21,22] and BrCl[13,21-23] from data recorded at 298 K and recently applied to CF_3I[24] at six temperatures between 218 and 333 K.

Alternatively, Joens[25,26] has proposed a method based on linear Gaussian distribution functions to describe the shapes and predict the temperature dependencies of UV absorption continua:

$$\sigma(T) = \sigma_{med}(T) \frac{\tilde{\nu}}{\tilde{\nu}_{med}(T)} \exp\left\{-\left[\frac{\tilde{\nu} - \tilde{\nu}_{med}(T)}{\Delta\tilde{\nu}(T)}\right]^2\right\} \qquad (2)$$

where $\sigma_{med}(T) = hB\tilde{\nu}_{med}(T)/[\sqrt{\pi}\Delta\tilde{\nu}(T)]$; $\tilde{\nu}_{med}(T) = U'_{\tilde{\xi}=0} - \omega_e''$ coth/4; $\Delta\tilde{\nu}(T) = \sqrt{(\omega_e''\text{coth}/2)^2 + \beta^2\,\text{coth}}$; and coth = $\coth[hc_0\omega_e''/(2kT)]$.

In eq 2 the cross section and the wavenumber at the median absorption, $\sigma_{med}(T)$ and $\tilde{\nu}_{med}(T)$, and the breadth parameter $\Delta\tilde{\nu}(T)$ are determined by fitting and, where more than one reaction component absorbs, deconvolution in an appropriate number of individual bands. Provided that the harmonic vibrational wavenumber ω_e'' is known, the Einstein absorption coefficient B[14,15] and the parameters $U'_{\tilde{\xi}=0}$ and β, the physical meaning of which will be explained below (*cf.* eq 7), can be computed. This allows the shape of an UV absorption continuum to be predicted via eq 2 for any arbitrary temperature for which the underlying assumptions are reasonably valid. Finally, note that in eq 2 the median absorption coincides with the mean wavenumber defined via $\tilde{\nu}_{mean} = (hB)^{-1}\int_0^{\infty}\sigma(T)\, d\tilde{\nu}$ but not with the maximum absorption, in contrast to eq 1.

The methods for modeling the temperature dependence are independent of whether the band shape is approximated via a linear or a semilogarithmic Gaussian distribution function. Consequently, the method proposed by Joens[25,26] and used in eq 2 can also be combined with eq 1:

$$\sigma(T) = \sigma_{max}(T) \exp\{-a(T)[\ln(\tilde{\nu}/\tilde{\nu}_{max}(T))]^2\} \qquad (3)$$

where $\sigma_{max}(T) = hB\sqrt{a(T)/\pi}$; $\tilde{\nu}_{max}(T) = (U'_{\tilde{\xi}=0} - \omega_e''\,\text{coth}/4)/\sqrt{Z}$; $a(T) = 0.5/\ln(Z)$; $Z = 1 + 0.5[(\omega_e''\text{coth}/2)^2 + \beta^2\,\text{coth}]/(U'_{\tilde{\xi}=0} - \omega_e''\,\text{coth}/4)^2$; and coth = $\coth[hc_0\omega_e''/(2kT)]$.

Joens[27] recently proposed that eq 2 is well suited for describing the shapes and predicting the temperature dependencies of the absorption continua of $HO_2^{\bullet}$ between 300 and 1100 K, $CH_3O_2^{\bullet}$ between 300 and 662 K and $CH_3CH_2O_2^{\bullet}$ between 300 and 600 K. In contrast, eq 3 is novel and has not yet been used. One of the objectives of this work is to compare and assess eqs 1−3 using the absorption continua of $CH_3CH_2O_2^{\bullet}$[8,9] and $CH_3O_2^{\bullet}$[1,2,10] as examples, because the performance of semilogarithmic and linear Gaussian distribution functions has hitherto not been compared for peroxy radicals.[1,17-20,27] A theoretical comparison will also be given and a potential energy diagram as a function of the photoexcitation coordinate will be computed from the fit parameters. The usefulness of Gaussian distribution functions for detecting unexpected features in the shapes of experimentally determined absorption continua will be demonstrated using the example of $HO_2^{\bullet}$.[16]

3. Comparison of Eqs 1 and 2

The simplest means to compare the appropriateness of eqs 1 and 2 for describing the shapes and predicting the temperature dependencies of the $HO_2^{\bullet}$ and $RO_2^{\bullet}$ absorption continua is to compare the figures of Joens'[27] paper, which are based on eq 2, with the corresponding figures based on eq 1. Such a comparison is possible only for $CH_3CH_2O_2^{\bullet}$, for which Fenter *et al.*[9] obtained better fits using eq 1 in combination with the absorption cross sections they recorded at 298 and 600 K (Figure 2 in ref 9) than Joens[27] using eq 2 in combination with the absorption cross sections recorded by Bauer *et al.*[8] at 298 K (Figure 4 in ref 27). We have repeated the fits for the example of $CH_3CH_2O_2^{\bullet}$ using the absorption cross sections reported by Bauer *et al.*[8] and Fenter *et al.*[9]

Figure 1 shows the best fits of eqs 1 and 2 to the absorption cross sections of $CH_3CH_2O_2^{\bullet}$ recorded by Bauer *et al.*[8] at 298 K. Because the scatter of the experimental data is uniform throughout the wavelength range studied, unweighted fitting was preferred such that $\sum(\sigma_{expl} - \sigma_{fitted})^2$ was minimized,[28] where σ denotes the absorption cross section. As can be seen from

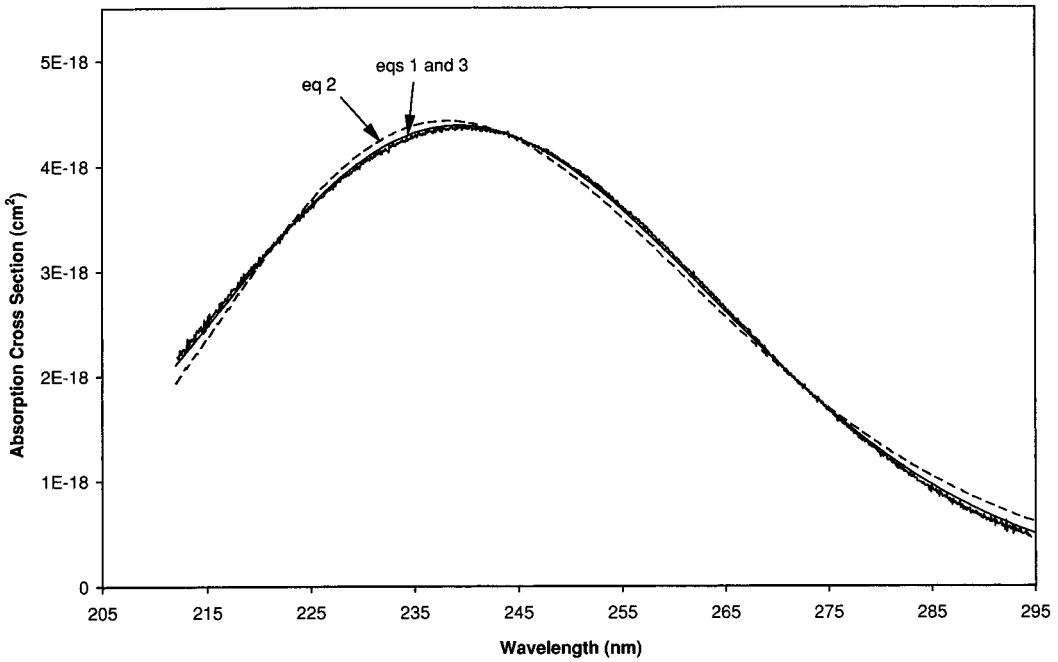

Figure 1. Best fits of eqs 1, 2, and 3 to the absorption cross sections of $CH_3CH_2O_2^•$ recorded by Bauer *et al.*[8] at 298 K (Std = 3.5×10^{-20} cm^2, 9.9×10^{-20} cm^2, and 3.5×10^{-20} cm^2, respectively).

TABLE 1: Values of the Parameters of Eqs 1−3 Obtained in the Best Fits to the Absorption Cross Sections of $CH_3CH_2O_2^•$ Recorded by Bauer *et al.*[8] at 298 K

		fit	assuming that $\omega_e'' = 1112$ cm^{-1} [1]	
eq 1	σ_{max}(298 K)	$(4.3868 \pm 0.0019) \times 10^{-18}$ cm^2	$\sigma_{max}(0)$	4.407×10^{-18} cm^2
	$\tilde{\nu}_{max}$(298 K)	$41\,783.6 \pm 2.5$ cm^{-1}	$\tilde{\nu}_{max}(0)$	$=\tilde{\nu}_{max}$(298 K)
	a(298 K)	49.776 ± 0.068	$a(0)$	50.24
eq 2	σ_{med}(298 K)	$(4.4098 \pm 0.0056) \times 10^{-18}$ cm^2	B	1.632×10^{11} s kg^{-1}
	$\tilde{\nu}_{med}$(298 K)	$41\,574.5 \pm 6.4$ cm^{-1}	$U'_{\xi=0}$	41 855 cm^{-1}
	$\Delta\tilde{\nu}$(298 K)	5754 ± 11 cm^{-1}	β	5700 cm^{-1}
eq 3	the same as for eq 1		B	1.663×10^{11} s kg^{-1}
			$U'_{\xi=0}$	42 275 cm^{-1}
			β	5913 cm^{-1}

Figure 1, eq 1 fits the experimental data slightly better than eq 2. For a quantitative comparison, the standard deviations of the fits defined via $\text{Std} = [\sum(\sigma_{expl} - \sigma_{fitted})^2/(n-m)]^{0.5}$,[28] where n is the number of fitted experimental absorption cross sections and m is the number of adjustable parameters, are given in the figure caption. Note that $m = 3$ in the case of eqs 1 and 2. The values of the fit parameters are listed on the left-hand side of Table 1. On the right-hand side values computed assuming a harmonic vibrational wavenumber corresponding to the O−O stretching vibration, $\omega_e'' = 1112$ cm^{-1},[1] are given. The latter is the most plausible approximation for the photoexcitation coordinate of $CH_3CH_2O_2^•$. This result, that semilogarithmic Gaussian distribution functions approximate the shapes of UV−visible absorption continua better than their linear analogues, was also observed for Cl_2[11,13] and BrCl[13,23] at 298 K.

Figure 2 shows the best fits of eqs 1 and 2 to the absorption cross sections of $CH_3CH_2O_2^•$ recorded by Fenter *et al.*[9] at 298 and 600 K. Both spectra were fitted simultaneously assuming, as before, that $\omega_e'' = 1112$ cm^{-1}.[1] In eq 1 the fit parameters were σ_{max}(298 K), σ_{max}(600 K), $\tilde{\nu}_{max}$, and $a(0)$, the σ values being uncorrelated because of the experimental uncertainty in their ratio.[9] In eq 2 the fit parameters were σ_{med}(298 K), σ_{med}(600 K), $U'_{\xi=0}$, and β, the σ values being again uncorrelated. Thus in each fit the number of adjustable parameters equaled $m = 4$. Weighted fitting was used such that $\sum[(\sigma_{exptl} - \sigma_{fitted})/\text{Std}_{exptl}]^2$ was minimized,[28] where Std_{exptl} denotes the standard deviations of the experimental absorption cross sections.[9] As can be seen from Figure 2, at both temperatures eq 1 approximates the shape of the absorption continuum of $CH_3CH_2O_2^•$ better than eq 2. For a quantitative comparison, the figure caption includes the standard deviations of the fits that were computed via $\text{Std} = \{\sum[(\sigma_{exptl} - \sigma_{fitted})/\text{Std}_{exptl}]^2/[(1 - m/n)\sum\text{Std}_{exptl}^{-2}]\}^{0.5}$.[28] This result agrees with that based on the data of Bauer *et al.*[8]

The best fit of eq 3 to the absorption cross sections of $CH_3CH_2O_2^•$ recorded by Bauer *et al.*[8] at 298 K is identical to that of eq 1 shown in Figure 1. The values of the corresponding fit parameters are given on the left-hand side of Table 1, whereas those on the right-hand side were computed assuming again that $\omega_e'' = 1112$ cm^{-1}.[1]

Figure 2 shows the best fit of eq 3 to the absorption cross sections of $CH_3CH_2O_2^•$ recorded by Fenter *et al.*[9] at 298 and 600 K. Both spectra were fitted simultaneously assuming that $\omega_e'' = 1112$ cm^{-1}.[1] The fit parameters were σ_{max}(298 K), σ_{max}(600 K), $U'_{\xi=0}$, and β, the σ values being uncorrelated as in the above fits of eqs 1 and 2. The number of adjustable parameters was thus $m = 4$. The good agreement of the fit with that obtained using eq 1, *cf.* Figure 2, indicates that the methods used for modeling the temperature dependence are comparably good at least in the case of the UV continuum of $CH_3CH_2O_2^•$ in the temperature range between 298 and 600 K.

Equations 1−3 were also compared for the case of $CH_3O_2^•$ in a manner similar to that above using the room-temperature absorption cross sections recommended by Lightfoot *et al.*[1] and Wallington *et al.*[2] and those recorded by Lightfoot and Jemi-Alade[10] at 298 and 662 K. Unweighted fitting was used because for these data no error estimates have been reported.[1,2,10] The

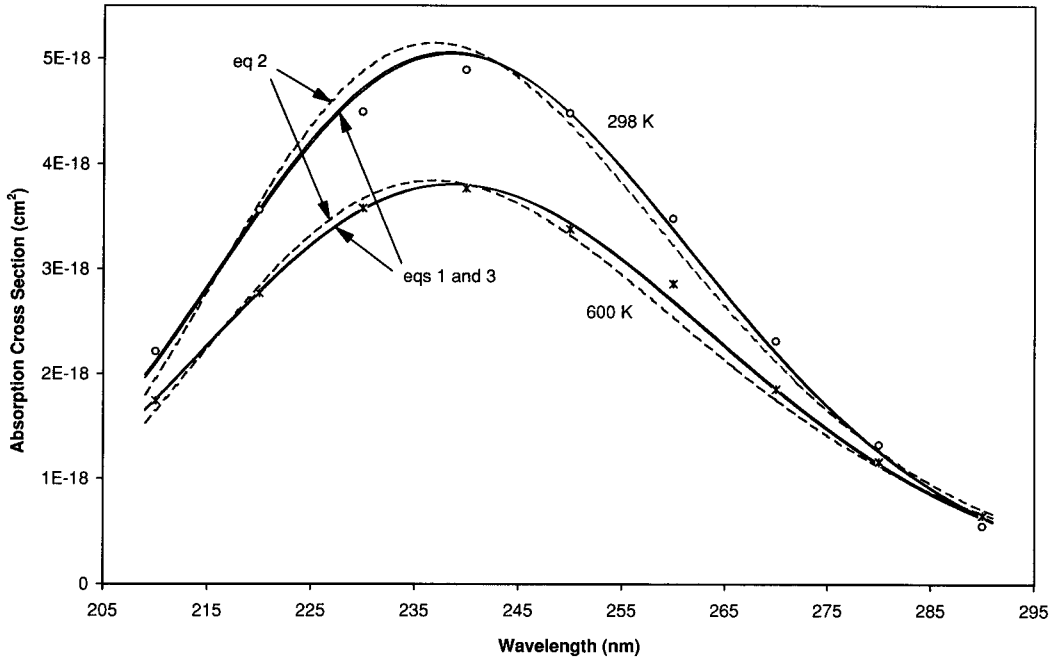

Figure 2. Best fits of eqs 1, 2, and 3 to the absorption cross sections of $CH_3CH_2O_2^{\bullet}$ recorded by Fenter *et al.*[9] at 298 K and 600 K (Std = 7.8×10^{-20} cm^2, 1.4×10^{-19} cm^2, and 7.5×10^{-20} cm^2, respectively).

TABLE 2: Standard Deviations (cm^2) of the Best Fits of Eqs 1−3 to the Absorption Cross Sections of $CH_3O_2^{\bullet}$[1,2,10]

reference	temperature	eq 1	eq 2	eq 3
Lightfoot *et al.*[1]	298 K	6.4×10^{-20}	1.1×10^{-19}	6.4×10^{-20}
Wallington *et al.*[2]	room temperature	1.8×10^{-19}	2.6×10^{-19}	1.8×10^{-19}
Lightfoot and Jemi-Alade[10]	298 and 662 K	1.5×10^{-19}	2.2×10^{-19}	1.3×10^{-19}

results of these fits are analogous to those for $CH_3CH_2O_2^{\bullet}$, as can be seen by comparison of the standard deviations given in Table 2 with those in the captions of Figures 1 and 2, and thus support the above conclusions about the suitability of eqs 1−3.

4. Theoretical Considerations

The approaches used for modeling the temperature dependence of eqs 1−3 are based on the method of spectral moments originally introduced by Lax[29] and recently elaborated in detail by Marić and Burrows.[13] For the definition of spectral moments *cf.* eq A-1 in the Appendix. In addition, they use the quasi-diatomic approximation, which assumes that the essential features of the multidimensional potential surfaces, between which an electronic transition takes place, can be represented by one-dimensional radial potentials as functions of a single photoexcitation coordinate ξ. They also assume the validity of the Condon[30,31] approximation that neglects the dependence of the electronic transition moment on the space coordinates or ξ, assuming it to be a constant. Finally, they assume a harmonic radial potential for the lower electronic state,

$$U'' = 0.5\omega''_e\xi^2 \qquad (4)$$

and neglect molecular rotation in order to use the analytical solution for the thermal average of the harmonic probability densities,[12,32] which simplifies the underlying mathematics, *cf.* the Appendix.

One means to quantify the suitability of eq 4 as an approximation for U'' is to allow the harmonic vibrational wavenumber for the lower electronic state, ω''_e, to vary during the fits to the absorption cross sections of $CH_3CH_2O_2^{\bullet}$ at 298 and 600 K.[9] This yielded $\omega''_e = 989 \pm 107$ cm^{-1} using eq 1 and $\omega''_e = 1043 \pm 105$ cm^{-1} using eq 3. The standard deviations of these fits were Std = 7.8×10^{-20} cm^2 and 7.6×10^{-20} cm^2, respectively, noting that the number of adjustable parameters was $m = 5$. Analogous results were also obtained for $CH_3O_2^{\bullet}$ at 298 and 662 K:[10] $\omega''_e = 977 \pm 175$ cm^{-1} with Std = 1.5×10^{-19} cm^2 using eq 1 and $\omega''_e = 954 \pm 144$ cm^{-1} with Std = 1.3×10^{-19} cm^2 using eq 3. For comparison, Lightfoot *et al.*[1] recommended $\omega''_e = 1112$ cm^{-1} for the O−O stretching vibration, which is the most plausible approximation for the photoexcitation coordinate of $CH_3CH_2O_2^{\bullet}$. The differences between the values of ω''_e obtained lie within the experimental error of the fitted absorption cross sections, indicating that eq 4 is an adequate approximation for U'' and that the O−O stretching vibration is representative of the photoexcitation coordinate ξ. Consequently, the value of ω''_e from ref 1 was used throughout this work. Incidentally, this value was also used by Joens.[27]

Equation 1 assumes an exponentially shaped difference between the radial potentials of the upper and lower electronic states:

$$\Delta U = U' - U'' = \tilde{\nu}_{max} \exp[-\xi/\sqrt{a(0)}] \qquad (5)$$

The radial potential for the upper electronic state, U', is obtained by adding ΔU to U''. However, a more realistic approximation for U'' than that given by eq 4 is needed to obtain a realistic U'.[13] In this work a Morse[33] radial potential was used:

$$U'' = D''_e[1 - \exp(\alpha\xi)]^2 \qquad (6)$$

where $D''_e = (\omega''_e)^2/(4\omega''_e x''_e)$ and $\alpha = \sqrt{2\omega''_e x''_e/\omega''_e}$. The vibrational anharmonicity constant was assumed to be $\omega''_e x''_e = 10$ cm^{-1}, in agreement with $\omega''_e x''_e = 10.6$ cm^{-1} which we have determined using data from a study on $HO_2^{\bullet}$ by Bunker *et al.*[34] For a Morse[33] radial potential the harmonic vibrational wavenumber equals $\omega''_e = \omega''_{v=1\leftarrow 0} + 2\omega''_e x''_e$, where $\omega''_{v=1\leftarrow 0} = 1112$

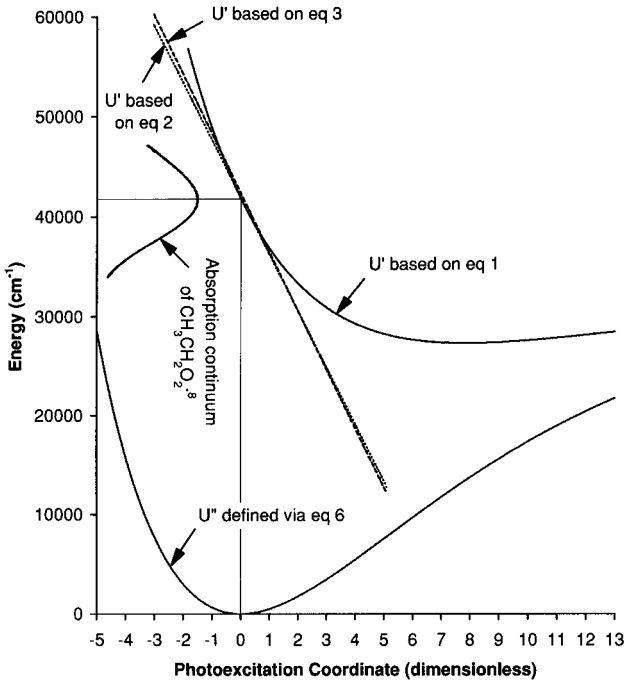

Figure 3. Potential energy diagram of $CH_3CH_2O_2^•$ as a function of the photoexcitation coordinate ξ.

cm^{-1}.[1] Otherwise throughout this work it was assumed that $\omega_e'' = \omega_{v=1\leftarrow 0}''$, which is a valid approximation for a harmonic radial potential.

Equations 2 and 3 are based on a linear radial potential for the upper electronic state:

$$U' = U'_{\xi=0} - \beta\xi. \tag{7}$$

where $U'_{\xi=0}$ and β are the position and the slope of the potential at $\xi = 0$, respectively.

Figure 3 shows the potential energy diagram of $CH_3CH_2O_2^•$ as a function of the photoexcitation coordinate ξ. The radial potential for the lower electronic state, U'', was computed via eq 6. The three representations of the radial potential for the upper electronic state, U', are based on the fit parameters of eqs 1−3 given in Table 1. U' based on the fit parameters of eq 1 was obtained by adding ΔU computed by eq 5 to U'' defined by eq 6, whereas U' based on the fit parameters of eqs 2 and 3 was computed by eq 7.

The similarity of the representations for U' in the Franck−Condon region (*i.e.* around the minimum of U'', *cf.* Figure 3) implies that the temperature dependencies of UV absorption continua predicted by eqs 1−3 are equal within experimental error for a narrow temperature range or a large value of ω_e''. This agrees with the results of the fits to the absorption cross sections of $CH_3CH_2O_2^•$, *cf.* Figure 2. However, outside this range eq 1 is more likely to predict the temperature dependencies correctly because it is based on a more realistically shaped U'.

The shallow minimum observed in Figure 3 for U' based on eq 1 deserves some attention. It is a result of the extrapolation of ΔU beyond the Frank−Condon region and its addition to U''. As shown by Tellinghuisen and Henderson,[35] the dissociation limit of U'' is usually overestimated when computed from ω_e'' and $\omega_e\chi_e''$ on the basis of a Morse[33] radial potential, *i.e.* eq 6.[35] Hence the lowering of the dissociation limit of U'' might eliminate the minimum in U'. However, eq 5 assumes that U'' and U' have identical dissociation limits, but according to a theoretical study by Vazquez *et al.*,[36] the corresponding states of $HO_2^•$ dissociate along the photoexcitation coordinate to $OH(X^2\Pi) + O(^3P)$ and $OH(X^2\Pi) + O(^1D)$, respectively. Provided that $CH_3CH_2O_2^•$ dissociates in an analogous manner, the dissociation limit of U' would be higher by 15 867 cm^{-1} than that of U''.[36] Consequently, the shallow minimum in U' of $CH_3CH_2O_2^•$ may be real and have one or more discrete vibrational levels.

The essence of the method of spectral moments, as used in the Appendix to derive the temperature dependencies of eqs 1−3, is to find a suitable distribution function that provides a realistic description for the shape of UV absorption continua and a realistic model potential such that both are characterized by the same number of adjustable parameters. The parameters of the distribution function can then be inverted to those of the potential and *vice versa* via the corresponding number of spectral moments. The infinite series of spectral moments defined by eq A-1 in the Appendix can thus be truncated assuming that the neglected moments do not contain any extra information.

For example, in the Appendix the electronic transition moment M, which is regarded as a parameter of the potential, and the two adjustable parameters of eq 5, $\tilde{\nu}_{max}$ and $a(0)$, are inverted using the zeroth, first, and second spectral moments to become the three adjustable parameters of eq 1, $\sigma_{max}(T)$, $\tilde{\nu}_{max}$, and $a(T)$. Coincidentally, $\tilde{\nu}_{max}$ turns out to be independent of temperature in this model. Similarly, M and the two adjustable parameters of eq 7, $U'_{\xi=0}$ and β, are inverted via the zeroth, first, and second spectral moments, yielding the three adjustable parameters of eq 2, $\sigma_{med}(T)$, $\tilde{\nu}_{med}(T)$, and $\Delta\tilde{\nu}(T)$, or those of eq 3, $\sigma_{max}(T)$, $\tilde{\nu}_{max}(T)$, and $a(T)$. The third and all higher spectral moments are in each case neglected. For details of the inversion see the Appendix.

The zeroth, first, and second spectral moments of eqs 1−3 provide the basis for the inversion and are therefore equal to those predicted from their model potentials, whereas the third and higher moments are not equal to those predicted. However, in contrast to eqs 2 and 3, eq 1 is additionally based on the reflection method III,[13] so that its third and higher moments are correct within the validity of this semiclassical method, *cf.* ref 13 and eq 48 therein. This means that the prediction of the temperature dependence by eq 1 will be superior to that by eqs 2 and 3.

5. Absorption Continuum of $HO_2^•$

In section 3 the suitability of eqs 1 and 2 for describing the shapes of the $RO_2^•$ absorption continua was contrasted by using accurate experimental absorption cross sections of $CH_3CH_2O_2^•$,[8,9] and eq 1 was found to be the most suitable. In addition, eq 1 was shown to describe adequately the shapes of the absorption continua of at least 19 $RO_2^•$ radicals in the gas phase[1,17−19] and that of $HOCH_2O_2^•$ in the aqueous phase,[20] *cf.* section 2. However, the absorption cross sections of $HO_2^•$ recorded by Crowley *et al.*[16] at 298 K cannot be described by eq 1 in terms of a single band, as noted by Lightfoot *et al.*[1] In this section the cause of the discrepancy is discussed.

Figure 4 shows the best fit of eq 1 to the absorption cross sections of $HO_2^•$ recorded by Crowley *et al.*[16] at 298 K. Weighted fitting was preferred. The standard deviation of the experimental absorption cross sections was estimated from their scatter and modeled as a function of the wavelength via $Std_{exptl}/cm^2 = 2.48 \times 10^{-20} + 3.64 \times 10^{-12} \exp(-8.53 \times 10^{-02}\lambda/nm)$. As can be seen from Figure 4, this spectrum cannot be adequately described by eq 1 in terms of a single band. This has four potential causes: (i) the shapes of the UV absorption

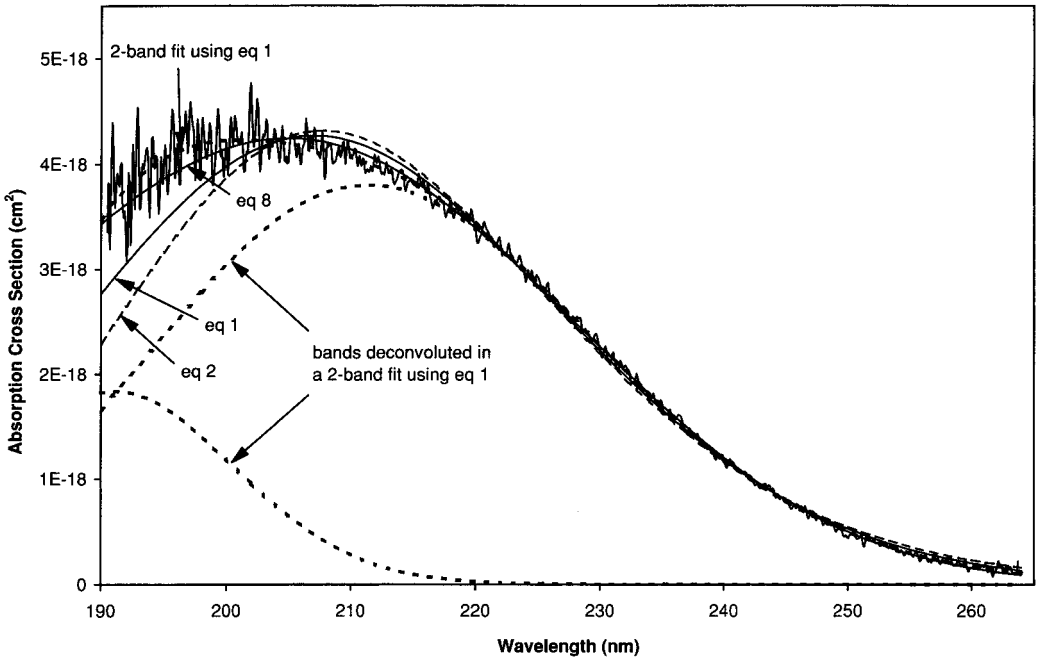

Figure 4. Best fits of eqs 1, 2, and 8 to the absorption cross sections of $HO_2^\bullet$ recorded by Crowley *et al.*[16] at 298 K (Std = 6.3×10^{-20} cm^2, 8.7×10^{-20} cm^2, and 4.5×10^{-20} cm^2, respectively). Also shown is a two-band fit of eq 1 and the bands deconvoluted in this manner (Std = 4.0×10^{-20} cm^2).

continua of $HO_2^\bullet$ and possibly other $RO_2^\bullet$ radicals are better described by eq 2, (ii) they are double-banded, (iii) they are strongly skewed, and (iv) the experimental absorption cross sections are erroneous, e.g. contaminated by the absorption of other reaction components or stray light.

The first possibility can be ruled out because eq 1 describes the shape of the studied absorption continuum[16] better than eq 2, as can be seen in Figure 4. The second explanation is improbable because the bands deconvoluted in a two-band fit of eq 1 having $m = 6$ adjustable parameters and shown in Figure 4 are inconsistent with the single-band absorption predicted by our present understanding of the $HO_2^\bullet$ and $RO_2^\bullet$ absorption continua. However, the existence of a weak absorption band in the short wavelength part of the $HO_2^\bullet$ spectrum cannot be ruled out.[7,36−38] It is also interesting to note that the absorption continuum of $HO_2^\bullet$ is shifted to shorter wavelengths as compared to $RO_2^\bullet$ radicals, *cf.* Figures 1, 2, and 4.

The third possibility was tested using an extended version of eq 1 proposed by Marić and Burrows:[13]

$$\sigma(T) = \frac{\sigma_{\text{med}}(T)}{1 - b(T)/\tilde{\nu}} \exp\left\{-a(T)\left[\ln\left(\frac{\tilde{\nu} - b(T)}{\tilde{\nu}_{\text{med}}(T) - b(T)}\right)\right]^2\right\} \quad (8)$$

For $b(T) = 0$ eq 8 reduces to eq 1. Consequently, the value of $b(T)$ is an indicator for the skewness of an UV absorption continuum, provided that it is adequately described by eq 8. Note that in eq 8 the number of adjustable parameters equals $m = 4$.

The best fit of eq 8 to the absorption cross sections of $HO_2^\bullet$ recorded by Crowley *et al.*[16] at 298 K yields $b(298\text{ K}) = 26\,816 \pm 374$ cm^{-1} and is shown in Figure 4. Compared to $\tilde{\nu}_{\text{med}}(298\text{ K}) = 49\,534 \pm 65$ cm^{-1}, this value is indeed far from zero, implying a pronounced skewness and thus in stark contrast to the other fitted absorption cross sections of $RO_2^\bullet$ radicals, *cf.* sections 2 and 3. This explanation is therefore considered unlikely.

Having excluded the first and third possibilities, the analysis indicates that either an unidentified electronic transition for $HO_2^\bullet$ around 190 nm is occurring or experimental error occurred in the determination of the absorption cross sections at short wavelengths resulting from contamination by other absorbing species or stray light. This work shows therefore, either that our understanding of the $HO_2^\bullet$ potentials and transitions is deficient or that the best available spectra are in error.

6. Summary

The suitability of eqs 1−3 for describing the shapes and temperature dependencies of the $RO_2^\bullet$ absorption continua has been studied using recent accurate measurements of the absorption cross sections of $CH_3CH_2O_2^\bullet$.[8,9] From comparisons with the experimentally determined spectra and theoretical considerations, eq 1 was found to be the most suitable. A procedure for computing potential energy diagrams as functions of the photoexcitation corrdinate from the fit parameters of eqs 1−3 was demonstrated. Analysis of the temperature dependence shows that the O−O stretching vibration approximates well the photoexcitation coordinate for $CH_3CH_2O_2^\bullet$. Analogous results obtained for $CH_3O_2^\bullet$[1,2,10] support the above conclusions. Reanalysis of the absorption continuum of $HO_2^\bullet$ indicates that either the measurements contain some contamination at short wavelengths or an unidentified electronic transition exists. This work demonstrates the usefulness of eq 1 in the analysis of UV spectra.

Acknowledgment. We are indebted to J. A. Joens, J. Tellinghuisen, and T. J. Wallington for helpful comments and K.-H. Möbus for the fitting program. This work was supported by the Institut für Sicherheitstechnologie, the Max-Planck-Gesellschaft, the University of Bremen, the EU environmental program, and the DARA.

Appendix: The Derivation of the Temperature Dependencies of Eqs 1−3

According to Lax,[29] the moments of an absorption band are given by

$$\langle\langle \tilde{\nu}^i \rangle\rangle_T = \int \sigma(T)\tilde{\nu}^i \, \mathrm{d}\ln(\tilde{\nu}) = \frac{2\pi^2}{3\epsilon_0 hc_0} \langle\langle M\psi''_{v,J} | \sum_{J'} S^{J'}_{J''} (H'_J - E''_{v,J})^i | M\psi''_{v,J} \rangle\rangle_T \quad \text{(A-1)}$$

where M is the electronic transition moment; $\psi''_{v,J}$ and $E''_{v,J}$ denote the normalized bound radial wave functions and the corresponding energies of the lower electronic state; $S^{J'}_{J''}$ are the normalized rotational line intensity factors; and H'_J is the radial Hamiltonian operator of the upper electronic state. For more details see ref 13.

Provided that M is constant (*i.e.* independent of the photoexcitation coordinate), as assumed by Condon,[30,31] and the Q-branch approximation,[6] which neglects the splitting in the P-, Q-, and R-branches, is assumed to be valid, the zeroth, first, and second spectral moments ($i = 0$, 1, and 2) reduce to[29,39]

$$\langle\langle \tilde{\nu}^i \rangle\rangle_T = \frac{2\pi^2 M^2}{3\epsilon_0 hc_0} \langle \Delta U^i \langle |\psi''_{v,J}|^2 \rangle_T \rangle \quad \text{(A-2)}$$

where $\Delta U = U' - U''$ is the difference between the upper and the lower radial potentials.

As shown by Ott[32] and independently by Sulzer and Wieland,[12] the thermal average of the harmonic probability densities is given by

$$\langle |\psi''_v|^2 \rangle_T = \sum_{v=0}^{\infty} N_v |\psi''_v|^2 = \sqrt{\tanh/\pi} \, \exp(-\xi^2 \tanh) \quad \text{(A-3)}$$

where ψ''_v denotes the normalized harmonic radial wave function of the lower electronic state of a nonrotating molecule; $N_v = \{1-\exp[-hc_0\omega''_e/(kT)]\} \times \exp[-hc_0\omega''_e v/(kT)]$ is the Boltzmann thermal population density of the vth vibrational level of a harmonic oscillator; $\tanh = \tanh[hc_0\omega''_e/(2kT)]$; ξ is the photoexcitation coordinate; and ω''_e is the harmonic vibrational wavenumber of the lower electronic state. Note that the neglect of molecular rotation, $J' = J'' = 0$, required by eq A-3 is a special case of the Q-branch approximation, $J' = J'' \geq 0$,[6] assumed in the derivation of eq A-2.

Combining eqs A-2 and A-3 yields for the zeroth, first, and second spectral moments

$$\langle\langle \tilde{\nu}^i \rangle\rangle_T = \frac{2\pi^2 M^2}{3\epsilon_0 hc_0} \sqrt{\tanh/\pi} \, \langle \Delta U^i \exp(-\xi^2 \tanh) \rangle \quad \text{(A-4)}$$

which, assuming that ΔU is defined by eq 5, yields

$$\langle\langle \tilde{\nu}^i \rangle\rangle_T = \frac{2\pi^2 M^2}{3\epsilon_0 hc_0} \tilde{\nu}^i_{\max} \exp\left[\frac{i^2 \coth}{4a(0)}\right] \quad \text{(A-5)}$$

Provided that $2\pi^2M^2/(3\epsilon_0 hc_0) = \sigma_{\max}(0)\sqrt{\pi/a(0)}$, this result is for all i identical to that obtained by integrating eq 1 as required by the definition of the spectral moments given in eq A-1. In this context, the reflection method III assumes that eqs A-2, A-4, and consequently A-5 are also valid for all i.[13]

Similarly, assuming that ΔU is equal to the difference between eqs 7 and 4, $\Delta U = U'_{\xi=0} - \beta\xi - 0.5\omega''_e\xi^2$, eq A-4 yields

$$\langle\langle \tilde{\nu}^i \rangle\rangle_T = \frac{2\pi^2 M^2}{3\epsilon_0 hc_0} \{(U'_{\xi=0} - \omega''_e \coth/4)^i + 0.5[(\omega''_e \coth/2)^2 + \beta^2 \coth]\delta_{i=2}\} \quad \text{(A-6)}$$

Because $2\pi^2M^2/(3\epsilon_0 hc_0) = hB$ for a constant M, where B is the Einstein absorption coefficient,[14,15] the above result is identical to that obtained for the zeroth, first, and second spectral moments by integrating eqs 2 and 3 as required by the definition of the spectral moments given in eq A-1.

References and Notes

(1) Lightfoot, P. D.; Cox, R. A.; Crowley, J. N.; Destriau, M.; Hayman, G. D.; Jenkin, M. E.; Moortgat, G. K.; Zabel, F. *Atmos. Environ.* **1992**, *26A*, 1805. Note that the authors preferred a semilogarithmic over a linear Gaussian distribution function because they were acquainted with ref 11 prior to publication and with some preliminary results of this work cited as being in preparation.

(2) Wallington, T. J.; Dagaut, P.; Kurylo, M. J. *Chem. Rev.* **1992**, *92*, 667.

(3) Levy, H., II. *Science* **1973**, *173*, 141.

(4) Crutzen, P. J. *Tellus* **1974**, *26*, 47.

(5) Crutzen, P. J. In *The Major Biogeochemical Cycles and Their Interactions*; Bolin, B., Cook, R. B., Eds.; SCOPE 21; J. Wiley: New York, 1983.

(6) LeRoy, R. J.; Macdonald, R. G.; Burns, G. *J. Chem. Phys.* **1976**, *65*, 1485.

(7) Langhoff, S. R.; Jaffe, R. L. *J. Chem. Phys.* **1979**, *71*, 1475.

(8) Bauer, D.; Crowley, J. N.; Moortgat, G. K. *J. Photochem. Photobiol. A: Chem.* **1992**, *65*, 329.

(9) Fenter, F. F.; Catoire, V.; Lesclaux, R.; Lightfoot, P. D. *J. Phys. Chem.* **1993**, *97*, 3530.

(10) Lightfoot, P. D.; Jemi-Alade, A. A. *J. Photochem. Photobiol. A: Chem.* **1991**, *59*, 1.

(11) Marić, D.; Burrows, J. P.; Meller, R.; Moortgat, G. K. *J. Photochem. Photobiol. A: Chem.* **1993**, *70*, 205.

(12) Sulzer, P.; Wieland, K. *Helv. Phys. Acta* **1952**, *25*, 653.

(13) Marić, D.; Burrows, J. P. *J. Phys. Chem.* **1996**, *100*, 8645.

(14) Einstein, A. *Phys. Z.* **1917**, *18*, 121.

(15) Füchtbauer, C. *Phys. Z.* **1920**, *21*, 322.

(16) Crowley, J. N.; Simon, F. G.; Burrows, J. P.; Moortgat, G. K.; Jenkin, M. E.; Cox, R. A. *J. Photochem. Photobiol. A: Chem.* **1991**, *60*, 1.

(17) Crowley, J. N.; Moortgat, G. K. *J. Chem. Soc., Faraday Trans.* **1992**, *88*, 2437.

(18) Catoire, V.; Lesclaux, R.; Lightfoot, P. D.; Rayez, M.-T. *J. Phys. Chem.* **1994**, *98*, 2889.

(19) Catoire, V.; Lesclaux, R.; Schneider, W. F.; Wallington, T. J. *J. Phys. Chem.* **1996**, *100*, 14356.

(20) Huie, R. E.; Clifton, C. L. *Chem. Phys. Lett.* **1993**, *205*, 163.

(21) Tellinghuisen, J. *J. Phys. Chem.* Submitted.

(22) Marić, D.; Burrows, J. P.; Moortgat, G. K. *J. Photochem. Photobiol. A: Chem.* **1994**, *83*, 179.

(23) Hubinger, S.; Nee, J. B. *J. Photochem. Photobiol. A: Chem.* **1995**, *86*, 1.

(24) Fahr, A.; Nayak, A. K.; Huie, R. E. *Chem. Phys.* **1995**, *199*, 275.

(25) Joens, J. A. *Chem. Phys. Lett.* **1987**, *138*, 512.

(26) Joens, J. A. *J. Phys. Chem.* **1993**, *97*, 2527.

(27) Joens, J. A. *J. Phys. Chem.* **1984**, *98*, 1394.

(28) Bevington, P. R. *Data Reduction and Error Analysis for the Physical Sciences*; McGraw-Hill: New York, 1969.

(29) Lax, M. *J. Chem. Phys.* **1952**, *20*, 1752.

(30) Condon, E. U. *Proc. Natl. Acad. Sci.* **1927**, *13*, 462.

(31) Condon, E. U. *Phys. Rev.* **1928**, *32*, 858.

(32) Ott, H. *Ann. Phys.* **1935**, *23*, 169.

(33) Morse, P. M. *Phys. Rev.* **1929**, *34*, 57.

(34) Bunker, P. R.; Hamilton, I. P.; Jensen, P. *J. Mol. Spectrosc.* **1992**, *155*, 44, Table II.

(35) Tellinghuisen, J.; Henderson, S. D. *Chem. Phys. Lett.* **1982**, *91*, 447.

(36) Vazquez, G. J.; Peyerimhoff, S. D.; Buenker, R. J. *Chem. Phys.* **1985**, *99*, 239, Figure 6.

(37) Shih, S.-K.; Peyerimhoff, S. D.; Buenker, R. J. *Chem. Phys.* **1978**, *28*, 299.

(38) Jafri, J. A.; Phillips, D. H. *J. Am. Chem. Soc.* **1990**, *112*, 2586.

(39) Adler-Golden, S. M. *Chem. Phys.* **1982**, *64*, 421.